Some Curious Phenomena in Coupled Cell Networks

Martin Golubitsky
Department of Mathematics
University of Houston
Houston TX 77204-3008, USA

Matthew Nicol
Department of Mathematics
University of Surrey
Guildford, Surrey GU2 5XH, UK

Ian Stewart
Mathematics Institute
University of Warwick
Coventry CV4 7AL, UK

December 7, 2003

Abstract

We discuss several examples of synchronous dynamical phenomena in coupled cell networks that are unexpected from symmetry considerations, but are natural using a theory developed by Stewart, Golubitsky, and Pivato. In particular we demonstrate patterns of synchrony in networks with small numbers of cells and in lattices (and periodic arrays) of cells that cannot readily be explained by conventional symmetry considerations. We also show that different types of dynamics can coexist robustly in single solutions of systems of coupled identical cells. The examples include a three-cell system exhibiting equilibria, periodic, and quasiperiodic states in different cells; periodic $2n \times 2n$ arrays of cells that generate 2^n different patterns of synchrony from one symmetry generated solution; and systems exhibiting multirhythms (periodic solutions with rationally related periods in different cells). Our theoretical results include the observation that reduced equations on a center manifold of a skew product system inherit a skew product form.

1 Introduction

In this paper we describe examples of surprising kinds of synchrony and dynamics that occur robustly in coupled cell networks as consequences of the network architecture. We focus mostly, though not entirely, on features of the network architecture that go beyond the symmetry of the network.

Such behavior will arise in real networks with the appropriate architecture if a model using coupled differential equations is accurate enough. On the other hand, exotic behavior

may occur in models because of apparently harmless modeling assumptions. In the absence of any obvious symmetry or other 'non-generic' features of the network, the role of these assumptions in generating the observed dynamics can easily be overlooked. For either reason, it is useful to have some understanding of how network architecture affects typical dynamics. This paper illustrate a selection of these exotic dynamical phenomena, and goes some way toward explaining them.

We define a *cell* to be a finite-dimensional system of differential equations on a phase space $\mathbf{R}^k$. A *coupled cell network* $\mathcal{C}$ consists of N cells whose equations are coupled. The *phase space* of $\mathcal{C}$ is $P = \mathbf{R}^{k_1} \times \cdots \times \mathbf{R}^{k_N}$. A *coupled cell system* has the form

$$\dot{x}_i = f_i(x) \qquad 1 \leq i \leq N$$

where $x_i \in \mathbf{R}^{k_i}$ and $f_i : P \to \mathbf{R}^{k_i}$. The *architecture* of a coupled cell system is a graph that indicates which cells are coupled, which cells have the same phase space, and which couplings are identical. A formal theory of coupled cell networks is developed in [13, 12]. General internal dynamics and coupling are permitted in this theory. A theory of weak coupling in the presence of symmetry is discussed in Ashwin and Swift [2] and Brown *et al.* [3].

A coupled cell system is *homogeneous* if all cells have the same internal dynamics and receive identical inputs from the same number and types of cells. In the diagram of a homogeneous network we depict all cells using the same symbol (such as a square or circle), and all edges using the same style of arrow. For example, the networks in Figure 1 (left, center) are homogeneous, whereas the network in Figure 8 is not. Most networks considered in this paper are homogeneous.

Robust polysynchrony and balanced relations. A *polysynchronous subspace* is a subspace of the phase space P of a coupled cell network, in which cell coordinates x_i are equal on specified (disjoint) subsets of cells. A polysynchronous subspace is *robustly polysynchronous* if it is flow-invariant for every coupled cell system with the given network architecture. For example, the diagonal $x_1 = \cdots = x_N$ is always robustly polysynchronous in a homogeneous cell network. Fixed-point subspaces of the group of network symmetries are well-known to be flow-invariant [11, 9] and provide one way, though *not* the only way, to obtain robustly polysynchronous subspaces.

In fact, all robustly polysynchronous subspaces can be characterized combinatorially. Suppose that the cells in a network of identical cells are colored (where the colors represent the classes of an equivalence relation). Following [13, 12] we say that the coloring is *balanced* if each cell of a given color receives inputs from cells with the same set of colors, including multiplicity. For example, the coloring of the 12-cell ring shown in Figure 1 (right) is balanced, because each black cell receives inputs from two black cells and two white cells, and each white cell receives inputs from two black cells and two white cells. However, the same coloring of the ring in Figure 1 (left) is not balanced: some black cells receive inputs from two black cells, while others receive inputs from one black cell and one white cell. It is proved in [13, Theorem 6.5] that a polysynchronous subspace is robustly polysynchronous

if and only if the cell network coloring given by coloring cells that are equal with the same color is balanced. In fact, the general case of inhomogeneous networks is treated in that theorem, with the same result. Balanced equivalence relations are shown to lead to robustly polysynchronous subspaces by verifing that the differential equations associated to each cell of a given color are identical when restricted to the polysynchronous subspace. The converse requires more effort.

Balanced relations and quotient networks. In Section 5 of [13] it is shown that the restriction of every coupled cell system to a robust polysynchronous subspace is itself a coupled cell system corresponding to a 'quotient network.' This statement is further refined in [12] to the following construction. Given a balanced coloring, form the *quotient network* whose cells are enumerated by the colors in the balanced relation, and whose arrows are the projections of arrows in the original network to the quotient network. More precisely, the number of arrows from color 1 to color 2 (the colors represent cells in the quotient) is the number of arrows from cells of color 1 in the original network to one cell of color 2 in that network. The three-color balanced relation in Figure 6 (left) whose quotient network is shown in Figure 7 provides a good example. A principal theorem in [12] states that every coupled cell system on a quotient network lifts to a coupled cell system on the original network. It follows that generic or typical behavior in the quotient network lifts to generic behavior in the polysynchronous subspace. We will use this result to prove that certain codimension one bifurcations on the quotient network (namely those that yield desired pattern of synchrony) imply codimension-one bifurcations in the original network (to those same patterns).

Structure of the paper. As mentioned, polysynchronous subspaces are often generated by symmetry groups (since fixed-point subspaces of symmetry groups are flow-invariant) — but not always. We begin by considering specific network architectures, motivated by the intriguing patterns of synchrony that they display, despite a lack of symmetry. In Section 2 we show that a 12-cell ring with nearest and next nearest neighbor identical couplings can exhibit patterns of synchrony that cannot be predicted by symmetry. Similarly, square arrays of cells with periodic boundary conditions and nearest neighbor coupling can lead to a huge number of synchronous solutions (in which the pattern of synchrony can have random features). This example is discussed in Section 3.

Multirhythms (time-periodic solutions where the frequencies exhibited in each cell are rationally related) can result from certain types of network architecture. Section 4 focuses on coupled rings and the symmetry group of the network to prove the existence of multirhythm solutions. The tool we use is the H/K Theorem [4, 9].

Certain network architectures can force solutions that exhibit different dynamical characteristics in different cells. We analyze a three-cell feed-forward network in Sections 5 and 6 that illustrates this point. We first show that the existence of synchrony-breaking bifurcations in codimension one that have nilpotent normal forms. The nilpotency is a straightforward consequence of a feed-forward network. In ordinary Hopf bifurcation it is well known that the amplitude of the bifurcating branch of periodic solutions grows as order

$\lambda^{\frac{1}{2}}$, where λ is the deviation of the bifurcation parameter from criticality. We show that in a three-cell feed-forward network, codimension-one Hopf bifurcation can lead to stable periodic solutions that are in equilibrium in cell 1 and periodic in cells 2 and 3 with the same period. The amplitude of the solution in cell 2 grows at the expected rate of $\lambda^{\frac{1}{2}}$, whereas the amplitude of the solution in cell 3 grows at the unexpected rate of $\lambda^{\frac{1}{6}}$. Section 6 shows that a secondary bifurcation can lead to solutions that are in equilibrium in cell 1, periodic in cell 2, and quasiperiodic in cell 3.

In the final two sections we point to curious features of coupled cell systems that do not currently have adequate explanations. Section 7 gives an example of a network that is in no sense feed-forward, but which nevertheless leads naturally to nilpotent linearizations in codimension one synchrony-breaking bifurcations. Neither the dynamical consequences of these nilpotent linearizations nor the network architectural reasons for their existence are yet understood. Section 8 presents results from simulation of a system of two unidirectional rings coupled through a 'buffer cell', where solutions *appear* to be rotating waves in each ring with a well-defined frequency for each ring — but with incommensurate frequencies in the two rings. Actually, appearances are deceptive, but experimental observations may give that impression.

The main point of this paper is to present diverse examples which illustrate the implications of network architecture for the nonlinear dynamics of coupled cell systems.

We use the following notation for certain standard finite groups: $\mathbf{Z}_n$ is the *cyclic* group of order n (and the symmetry group of a directed ring of n cells); $\mathbf{D}_n$ is the *dihedral* group of order $2n$ (and the symmetry group of a birectional ring of n cells); and $\mathbf{S}_n$ is the *permutation* group on n symbols of order $n!$ (and the symmetry group of an all-to-all coupled n cell system).

2 Patterns in Rings

Our first example is a bidirectional ring of twelve cells with nearest neighbor and next nearest neighbor identical coupling. See Figure 1 (center). More generally, let G_N be a bidirectional ring of N cells with nearest neighbor and next nearest neighbor coupling. That is, label the cells by elements of $\mathbf{Z}_N$ and couple cell i to cells $i-2, i-1, i+1, i+2$, with all arrows identical. System of differential equations corresponding to this graph have the form

$$\dot{x}_i = f(x_i, \overline{x_{i+1}, x_{i+2}, x_{i-1}, x_{i-2}}) \tag{2.1}$$

for $0 \leq i \leq N-1$, where the overline indicates that f is invariant under permutation of the last four arguments. We take $N \geq 5$ to avoid multiple arrows.

It is well-known that fixed-point subspaces are flow-invariant in symmetric systems [11, 9]. We will shortly prove the plausible fact that that both rings in Figure 1 (left, center) have the same symmetry group $\mathbf{D}_{12}$. This implies that they both have several robustly polysynchronous subspaces that are forced by symmetry. However, we show that the 12-cell ring with next nearest neighbor coupling supports a robust pattern of synchrony that

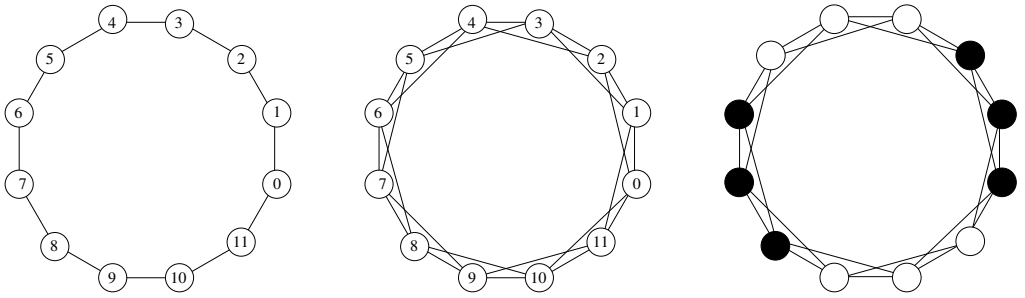

Figure 1: Twelve-cell bidirectional rings. (Left) nearest neighbor coupling. (Center) Nearest and next nearest neighbor coupling. (Right) A balanced equivalence relation on G_{12}.

is not determined by the $\mathbf{D}_{12}$ symmetry group, namely, the one shown in Figure 1 (right). In contrast, the 12-cell ring with nearest neighbor coupling does not support this pattern robustly. The distinction arises because the symmetry groupoids [13] are different in the two networks, and the ring G_{12} with next nearest neighbor coupling has a balanced equivalence relation that is not balanced for the ring with nearest neighbor coupling.

The *automorphism group* of a directed graph consists of all permutations of the cells that preserve arrows (and any labels for cell type or arrow type.) It is trivial to prove that the automorphism group of the nearest-neighbor ring is the obvious group $\mathbf{D}_{12}$. In Lemma 2.1 below we prove that when $N \geq 7$ the same is true for the automorphism group $\mathrm{Aut}(G_N)$. This result is presumably well known, but we have not found an explicit statement in the literature.

We now continue with the example. The subspace

$$W = \{(x, x, x, y, y, y, x, x, x, y, y, y)\}$$

is robustly polysynchronous in the network of Figure 1 (center) but not in Figure 1 (left). This is because the coloring of the ring with both nearest and next nearest neighbor coupling pictured in Figure 1 (right) is balanced, whereas the corresponding coloring when next nearest neighbor couplings are deleted is not balanced. Now [13, Theorem 6.5] implies that the space W is robustly polysynchronous in Figure 1 (right) only.

This pattern of synchrony has a striking structure, but it does not arise from the fixed-point space of a subgroup of $\mathbf{D}_{12}$. In fact, the subgroup H of $\mathbf{D}_{12}$ that fixes a generic point in W (that is, fixes the pattern) has order 4 and is generated by two reflections in orthogonal diameters of the ring. However, the fixed-point subspace of this subgroup

$$\mathrm{Fix}(H) = \{(x_1, x_2, x_1, y_1, y_2, y_1, x_1, x_2, x_1, y_1, y_2, y_1)\}$$

has dimension 4, not 2. In particular, in that fixed-point subspace, the central cell in each block of three does not have the same color as its two neighbors.

We can think of the 12-cell ring as the 'double cover' of the corresponding 6-cell ring. Indeed, there is a quotient map from G_{12} to G_6 in which cells $i, i+6$ map to cell i for $i = 0, \ldots, 5$. The corresponding pattern in G_6 corresponds to the polydiagonal $\{(x, x, x, y, y, y)\}$.

However, the exceptional nature of $\mathrm{Aut}(G_6)$ (see Lemma 2.1) implies that this space *is* the fixed-point space of a subgroup of $\mathrm{Aut}(G_6)$.

There are many similar examples. In G_{10} the subspace

$$\{(x,x,y,x,y,x,x,y,x,y)\}$$

corresponds to a balanced equivalence relation that is not balanced on a nearest-neighbor ring; this pattern does not arise from the fixed-point space of a subgroup of $\mathbf{D}_{10}$ (although the corresponding pattern (x,x,y,x,y) does arise in that manner in the quotient network G_5). The same goes for the pattern (x,x,x,y,y,x,x,x,y,y). With more than two colors, numerous examples can be devised.

Stable equilibria can exist in any polysynchronous subspace. Suppose that a coupled network of N identical cells has a robust polysynchronous subspace V. We remark here that there exists an asymptotically stable equilibrium in V for some admissible coupled cell system. In fact, we can choose this system to be affine linear. Let X_0 be in V and define $f(X) = X_0 - X$. Then $f(X_0) = 0$ and f is admissible (see results in [13]). Since $(Df)_{X_0} = -I$, the equilibrium at X_0 is asymptotically stable.

Existence of polysynchronous equilibria in W by primary bifurcation. The cell equations (2.1) restricted to W in the network in Figure 1 (center) have the form

$$\begin{aligned} \dot{x} &= f(x, \overline{y,y,x,x}) \\ \dot{y} &= f(y, \overline{x,x,y,y}) \end{aligned}$$

where the overline indicates that f is invariant under permutations in the last four variables. Using this form we show that equilibria lying in W can arise from a fully synchronous equilibrium by a primary steady-state bifurcation. This calculation can be performed on the flow-invariant subspace W.

For simplicity assume that the phase space for each cell is one-dimensional. Let J be the Jacobian of the cell system at a synchronous equilibrium restricted to W. Then

$$J = \begin{bmatrix} A+2B & 2B \\ 2B & A+2B \end{bmatrix}$$

where A the linearized internal dynamics and B is the linearized coupling. Then the eigenvalues of J are $A+4B$ and A with eigenvectors $(1,1)^t$ and $(1,-1)^t$, respectively. Suppose that the eigenvalue A moves through 0 with nonzero speed as a parameter is varied. Then, because the eigenvector has unequal components, the branch of bifurcating equilibria will have unequal coordinates in W and correspond to the desired pattern.

Computation of $\mathrm{Aut}(G_N)$.

Lemma 2.1 *Let $G_N, N \geq 5$ be a bidirectional ring of N cells with nearest neighbor and next nearest neighbor coupling. Then its automorphism group is:*

(a) $\mathrm{Aut}(G_N) = \mathbf{D}_N$ *if* $N \geq 7$.

(b) $\mathrm{Aut}(G_5) = \mathbf{S}_5$.

(c) $\mathrm{Aut}(G_6) = \langle \mathbf{D}_6, (03), (14) \rangle$ *(is of order 48).*

Proof Suppose for a contradiction that $\mathrm{Aut}(G_N)$ contains a permutation $\sigma \notin \mathbf{D}_N$. By composing σ with a suitable element of $\mathbf{D}_N$ we may assume, without loss of generality, that $\sigma(0) = 0$ and $\sigma(1) = 1$. Let K be a sequence of consecutive elements of $\mathbf{Z}_N$ (in cyclic order) that contains $0, 1$ and is maximal subject to $\sigma(k) = k$ for all $k \in K$. Composing with a suitable rotation in $\mathbf{D}_N$ we may assume that

$$K = \{0, 1, \ldots, k\}$$

We claim that when $N \geq 7$ we must have $K = \mathbf{Z}_N$, in which case $\sigma = \mathrm{id} \in \mathbf{D}_N$, a contradiction. Specifically, we prove by induction on $|K|$ that if $k < N - 1$ then K is not maximal.

We know that K contains $0, 1$. Suppose that $|K| = 2$ so $K = \{0, 1\}$. The only cells that connect to both 0 and 1 are $-1, 2$ and these are distinct since $N \geq 5$. Therefore $\sigma(2) = -1$ and $\sigma(-1) = 2$. Now cell 3 connects to both cells 1 and 2, so $\sigma(3)$ connects to both cells -1 and 1. When $N \geq 7$ the only such cell is cell 0, so $\sigma(3) = 0$ contrary to σ being a bijection.

Next, suppose that $|K| = 3$. Cell 3 connects to cells 1 and 2, so $\sigma(3)$ also connects to cells 1 and 2. When $N \geq 7$ the only such cells are 0 and 3. Since σ is a bijection, we must have $\sigma(3) = 3$, contradicting maximality of K. The same argument, applied to cell $k + 1$, works when $|K| \geq 4$ and $K = \{0, 1, \ldots, k\}$. The assumption $N \geq 7$ is needed in the proof because extra connections exist for small rings with $N = 5, 6$. We now analyze these two cases, for completeness.

When $N = 5$ the graph G_5 is the complete graph on 5 nodes, so its automorphism group is the full symmetric group $\mathbf{S}_5$. When $N = 6$ the proof strategy permits an extra automorphism (0 3), together with its conjugates (1 4) and (2 5) by $\mathbf{D}_6$, and products of these (but nothing else). These three transpositions generate a group $\mathbf{Z}_2 \times \mathbf{Z}_2 \times \mathbf{Z}_2$. Now, the product (1 3)(1 4)(2 5) is the rotation $i \mapsto i + 6$ which lies in $\mathbf{D}_6$, so the group $\langle \mathbf{D}_6, (0\ 3), (1\ 4), (2\ 5) \rangle$ has order 48 and the generator (2 5) is redundant. □

3 Periodic Arrays

The notion of a balanced equivalence relation or coloring applies to the architecture of lattice dynamical systems, and is a powerful tool for determining patterns of synchrony not suggested by the group-symmetry approach. An investigation of admissible patterns in square arrays of coupled cells with Neumann boundary conditions (and their stability) is given from a symmetry viewpoint in Gillis and Golubitsky [7]. We consider here square arrays with nearest neighbor coupling and periodic boundary conditions; however, many of

the results from [7] are relevant. In related work, Chow *et al.* [5, 6] consider lattice arrays with nearest and next-nearest neighbor coupling.

Consider an $m \times m$ array of cells, with bidirectional nearest-neighbor coupling (horizontal and vertical coupling only) and periodic boundary conditions, as pictured in Figure 2. The symmetry group of such an array is the semidirect product $\Gamma = \mathbf{D}_4 \dot{+} \mathbf{Z}_m^2$. (This product is semidirect since some of the elements of $\mathbf{D}_4$ and $\mathbf{Z}_m^2$ do not commute.)

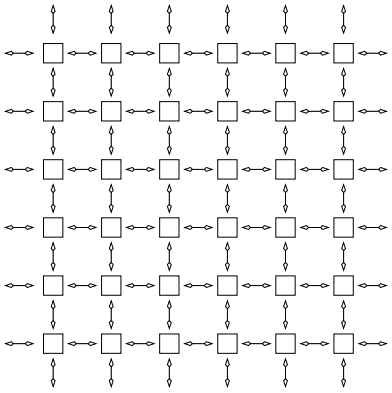

Figure 2: An $m \times m$ periodic array of cells.

We show that balanced coloring predicts the existence of equilibria with patterns of synchrony that have a certain kind of spatial randomness whenever a certain kind of regularly patterned equilibrium exists. We discuss both 2-color and 3-color balanced relations. The implications of balanced relations are not limited to dynamics consisting solely of equilibria. We also show that solutions in which there are time-periodic cells, some of which are half-a-period out of phase and some of which oscillate at twice the frequency, can occur naturally in periodic arrays.

Two-Color Balanced Relations

Equilibria. Periodic patterned states may be found in $4n \times 4n$ periodic lattices with two colors, as Figure 3 shows. The left figure is a 4-periodic balanced coloring with two colors: black and white. It is balanced because each cell receives two white and two black inputs. We note that this very regular pattern does not result from symmetry. To verify this point observe that the isotropy subgroup Σ of the pattern is generated by horizontal and vertical translations by 4 cells (the pattern is 4-periodic), by translation along the main northwest-southeast diagonals (the pattern has constant colors along diagonals), and by reflection across the main northeast-southwest diagonal. However, $\mathrm{Fix}(\Sigma)$ consists of 4-periodic patterns that have constant color along northwest-southeast diagonals; that is, the patterns in $\mathrm{Fix}(\Sigma)$ are generically four-color patterns.

Figure 3 (right) is another balanced coloring that results from the previous pattern by interchanging black and white along one northeast-southwest diagonal. More precisely, to generate the new equilibria, choose any diagonal that slopes upward to the right, such as the

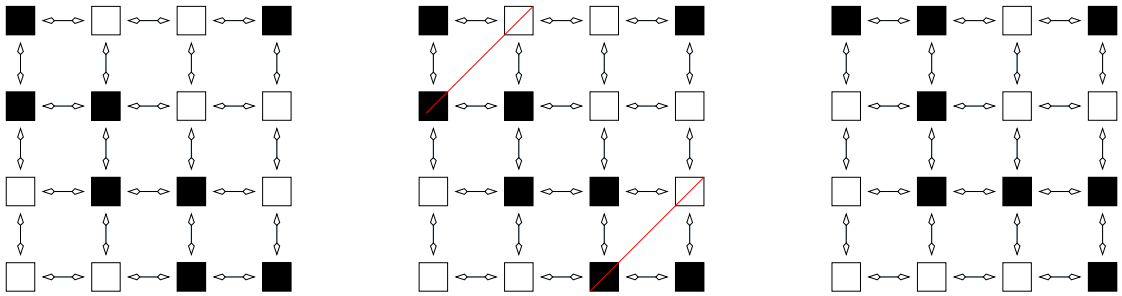

Figure 3: Two-coloring polysynchronous subspaces of a $4n \times 4n$ periodic array: (left) basic pattern; (center) specified diagonal; (right) new pattern.

one shown in Figure 3 (center). For cells on this diagonal change black to white and white to black. This new pattern of colors also gives rise to a balanced relation, Figure 3 (right). As before, the relation is balanced because every cell is coupled to two black cells and to two white cells.

The equations governing black x_B and white x_W cells in Figure 3 (left), where $x_B(t)$ and $x_W(t)$ are functions of time, are:

$$\begin{aligned} \dot{x}_B &= f(x_B, \overline{x_W, x_W, x_B, x_B}) \\ \dot{x}_W &= f(x_W, \overline{x_B, x_B, x_W, x_W}) \end{aligned} \tag{3.1}$$

since $f(x_1, \overline{x_2, x_3, x_4, x_5})$ is invariant under permutation of the last four variables; that is, all couplings are identical. In Figure 3 (right) the equations for the black cells all have the same form. Thus at each x_B site the same differential equation governs the behavior of the x_B cells in both Figure 3 (left) and Figure 3 (right). Similarly for white cells in both figures. Hence solutions of the coupled system are taken to solutions by the parity swap. Wang and Golubitsky [14] enumerate all two-color patterns of synchrony for square arrays.

It is well known that symmetry operations preserve stability of equilibria. However, parity swapping is not a symmetry operation and thus need not preserve the stability of solutions. Stability is preserved in the two-dimensional polysynchronous subspaces, but not in transverse directions.

Parity swapping along diagonals can lead to 16^n different equilibria. To see this, note that there are $4n$ diagonals in a $4n \times 4n$ array and two different equilibria are associated with each diagonal, thus yielding $2^{4n} = 16^n$ equilibria. Parity swaps can generate 'random' spatial patterns in the sense that along any selected vertical column there is a polysynchronous subspace that corresponds to an arbitrary sequence of black and white cells. In Figure 4 we illustrate the symmetric pattern on a 64×64 grid of cells and two different types of black and white interchanges on multiple diagonals.

Primary bifurcation to patterned equilibria. By (3.1) the restriction of the full coupled cell system to the two-color polysynchronous subspace is itself a two-cell system corresponding to the symmetric quotient network of Figure 5.

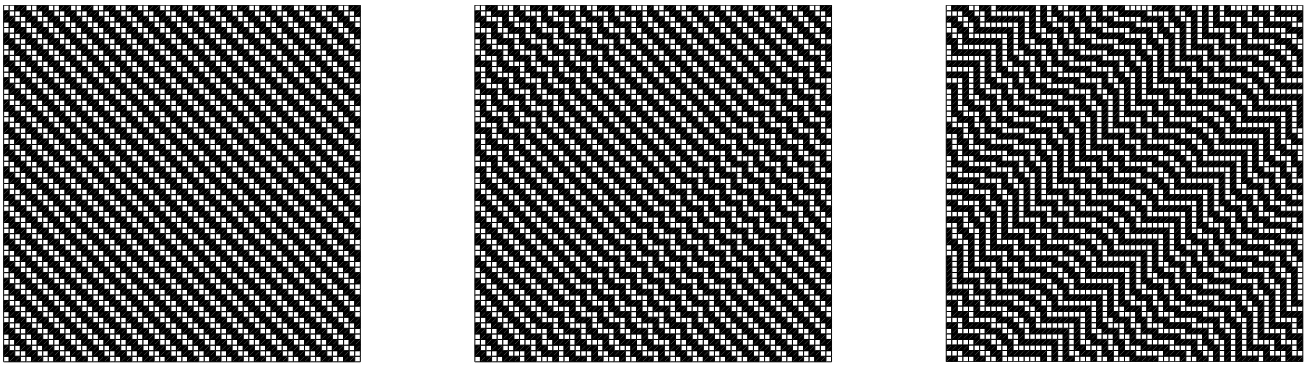

Figure 4: Polysynchronous subspaces of a 2-color 64×64 periodic array. (Left) The regular pattern. (Center) Dislocation pattern obtained by interchanging each 6^{th} diagonal. (Right) Interchanges on a random selection of 25 diagonals.

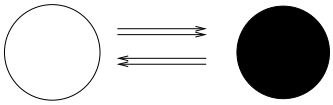

Figure 5: Quotient network for the 2-color balanced relations in Figures 3 and 4.

For simplicity, suppose that the phase space for each cell is one-dimensional. The fully synchronous subspace $x_B = x_W$ is flow-invariant, so the Jacobian of (3.1) at a synchronous state has an eigenvector in the direction $(1, 1)^t$ (where t is the transpose). By symmetry it also has one in the direction $(1, -1)^t$. It is straightforward to arrange that the eigenvalue associated with the symmetry-breaking eigendirection moves through zero with nonzero speed. Therefore a pitchfork bifurcation to the patterned solutions of Figure 3 will occur as a result of this codimension-one bifurcation.

Periodic states. Consider again the quotient network in Figure 5. The key observation about quotient networks is that coupled cell systems in the quotient network lift to coupled cell systems on the original network [12]. Moreover, this quotient network supports periodic solutions in which the left cell is half-a-period out of phase with the right cell. This solution can arise from Hopf bifurcation with two-dimensional internal dynamics [13]. Such a periodic solution lifts to any of the seemingly random 2-colorings of the lattice, giving rise to periodic solutions in which black cells are half-a-period out of phase with white cells.

Three-Color Balanced Relations

Equilibria. There is a 3-color balanced relation on a $2n \times 2n$ grid associated to the periodic symmetric pattern Figure 6 (left), so this pattern of synchrony corresponds to a robustly polysynchronous subspace. We first show that the existence of an equilibrium with this pattern of synchrony forces the coexistence of 2^n different equilibria with patterns of synchrony

that have a certain kind of randomness. Then we show that the symmetric equilibrium (and hence all of these equilibria) occurs naturally in primary bifurcations in such coupled cell arrays.

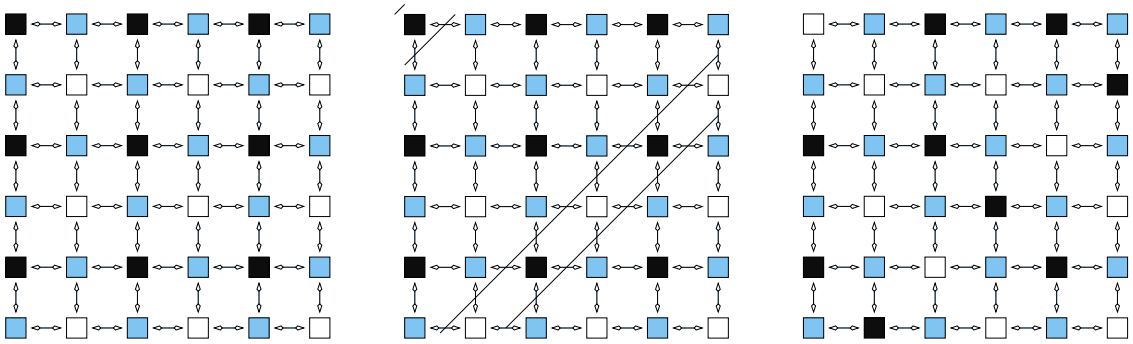

Figure 6: Three-color polysynchronous subspaces of a $2n \times 2n$ periodic array.

New equilibria by parity swap on a diagonal. Again we may choose any diagonal that slopes upward to the right and alternates black and white cells, and interchange black and white. This new pattern is also a balanced relation, Figure 6 (right). In both patterns, every black cell is coupled to four gray ones, every white cell is coupled to four gray ones, and every gray cell is coupled to two black and two white cells; so the relation is balanced. There are n diagonals that alternate black and white, and there are two choices of color on each diagonal, so there are 2^n different equilibria associated with this pattern of synchrony.

The differential equations governing black x_B, white x_W, and gray x_G cells in Figure 6 satisfy:

$$\begin{array}{rcl} \dot{x}_B & = & f(x_B, \overline{x_G, x_G, x_G, x_G}) \\ \dot{x}_W & = & f(x_W, \overline{x_G, x_G, x_G, x_G}) \\ \dot{x}_G & = & f(x_G, \overline{x_B, x_W, x_B, x_W}) \end{array} \tag{3.2}$$

since $f(x_1, \overline{x_2, x_3, x_4, x_5})$ is invariant under permutation of the last four variables. These equations are the same for both figures. Hence solutions of the coupled system are taken to solutions by the parity swap.

The three-color pattern is determined by symmetry. We begin by determining the isotropy subgroup $\Sigma \subset \Gamma$ of the symmetric pattern $\mathcal{P}$ illustrated in Figure 6 (left). The pattern $\mathcal{P}$ consists of 2×2 blocks repeated periodically, so Σ contains $\mathbf{Z}_n^2$, generated by the cell translations $(l, m) \mapsto (l + 2, m)$ and $(l, m) \mapsto (l, m + 2)$. Moreover, reflection ρ across the main diagonal, where $\rho(l, m) = (m, l)$, is a symmetry of $\mathcal{P}$. Indeed,

$$\Sigma = \mathbf{Z}_2(\rho) \dot{+} \mathbf{Z}_n^2$$

Since generic points in $\mathrm{Fix}(\Sigma)$ consists of states that have pattern $\mathcal{P}$, the pattern in Figure 6 (left) is determined by the subgroup Σ.

Primary bifurcation to the symmetric pattern. We now show that the pattern $\mathcal{P}$ may arise as a primary bifurcation from a fully synchronous equilibrium (where all cells are in the same state). For simplicity we assume that the phase space for each cell is one-dimensional. Denote the restriction (3.2) of the $4n^2$-dimensional coupled system to the three-dimensional polysynchronous subspace $\mathrm{Fix}(\Sigma)$ by $\dot{X} = F(X)$. A fully synchronous equilibrium satisfies $x_B = x_W = x_G$, which without loss of generality we may assume to be $(0,0,0)$. Denote the linearization $(DF)_0$ by L. A straightforward calculation shows that

$$L = \begin{bmatrix} \alpha & 0 & 4\beta \\ 0 & \alpha & 4\beta \\ 2\beta & 2\beta & \alpha \end{bmatrix} = \alpha I_4 + 2\beta \begin{bmatrix} 0 & 0 & 2 \\ 0 & 0 & 2 \\ 1 & 1 & 0 \end{bmatrix}$$

where α is the linearized internal dynamics of the cell and β is the linear coupling between cells. It is equally straightforward to check that the eigenvalues of L are: $\alpha + 4\beta$ with eigenvector $(1,1,1)^t$; $\alpha - 4\beta$ with eigenvector $(1,1,-1)^t$; and α with eigenvector $(1,-1,0)^t$.

It might seem surprising that the 3×3 matrix L always has real eigenvalues. This can be understood in several different ways. First, by direct calculation, as we have just done. Second, by observing that the one-dimensional subspace $x_B = x_W = x_G$ (this is $\mathrm{Fix}(\Gamma)$) and the two-dimensional subspace $x_B = x_W$ (this is $\mathrm{Fix}(\rho^\perp)$, where $\rho^\perp(l,m) = (2n+1-m, 2n+1-l)$) are flow-invariant. Hence, L must leave these subspaces invariant and have real eigenvalues. Finally, we recall from [12] that the restriction of a coupled cell system to a robust polysynchronous subspace is a coupled cell system on the associated quotient network. In this case the 3-color balanced coloring leads to the quotient network in Figure 7. Then the flow-invariant subspaces correspond to balanced colorings in the quotient network instead of to fixed-point subspaces of subgroups of the symmetry group Γ of the lattice. The multiarrows in Figure 7 reflect the fact that each gray cell receives two white and two black inputs, and each black and each white cell receives four gray inputs.

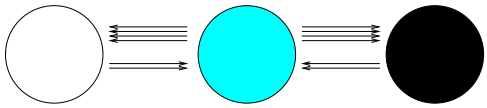

Figure 7: Quotient network for the 3-color balanced relations in Figure 6.

Returning to the bifurcation analysis, if (3.2) depends on a parameter λ and if $\alpha(\lambda)$ moves through 0 with nonzero speed, then a branch of equilibria will appear as generic points in $\mathrm{Fix}(\Sigma)$ (since the corresponding eigenvector is $(1,-1,0)^t$), and these equilibria will have pattern $\mathcal{P}$ in the original lattice. The bifurcation also breaks the $\mathbf{Z}_2$ symmetry ρ and therefore must be generically of pitchfork type.

Periodic states. The quotient system in Figure 7, with two-dimensional internal dynamics, supports Hopf bifurcation to a periodic solution in which the center cell has twice the frequency of the end cells and the end cells are half-a-period out of phase. Such a periodic

solution lifts to a periodic solution on the lattice with corresponding dynamics (gray cells at twice the frequency of white and black cells, which are half-a-period out of phase with each other).

Remark 3.1 Chow *et al.* [5, 6] study lattice dynamics and call solution patterns *mosaic patterns*. For a class of lattice differential equations with nearest neighbor and next nearest neighbor coupling, conditions for existence and stability of mosaic patterns have been obtained [5, Theorems 3.1, 3.2]. These conditions are specific to the particular site map of the lattice differential equation considered and phrased in terms of the parameters of the site map and the coupling strengths. Although there is some relation between the mosaic patterns and our 3-color patterns of synchrony (indeed, some of the patterns are identical), the results are quite different. Our results are model-independent, discuss nonequilibrium patterned states, do not allow next-nearest neighbor coupling, and do not include a stability analysis; the results of Chow *et al.* are model specific, apply only to equilibria, do allow longer range coupling, and do discuss stability.

4 Multirhythms

In this section we consider the phenomenon of multirhythms — hyperbolic periodic solutions whose projections in different cells have fundamental periods that are rationally, but not integrally, related. Our results in this section are based upon symmetry arguments and go against the grain of the rest of the paper, but for completeness we have included them here. Similar phenomena can occur in any network (possible asymmetric) that possesses a balanced equivalence relation whose quotient network is the same as the ones discussed here. (An example of a nonsymmetric network with a symmetric quotient is given in [13, Figure 6].) We will use the H/K theorem [4, 9] to show that multirhythms may be generated by cyclic symmetry of the coupled cell network.

Coupled cell dynamics can lead to situations where different cells are forced by symmetry to oscillate at different frequencies (Golubitsky and Stewart [8], Golubitsky *et al.* [11], Armbruster and Chossat [1]). In bidirectional rings, it is well known that certain cells can be forced by symmetry to oscillate at twice the frequency of other cells — but the range of possibilities is much greater. In general, the ratio of frequencies between cells of solutions whose existence is forced by symmetry need only be rational; when the ratio is a noninteger rational number, we call the periodic solution a *multirhythm*. We use the network pictured in Figure 8 as a first example and our exposition follows that in [10]. We then show that for each rational number r there is a coupled cell network that can exhibit multirhythms with frequency ratio r.

In symmetric systems with finite symmetry group Γ, the H/K theorem gives necessary and sufficient conditions for the existence of periodic solutions with prescribed spatio-temporal symmetries in some Γ-equivariant vector field.

Let $X(t)$ be a periodic solution of a Γ-equivariant system of ODE. Define

$$\begin{array}{rcl} K & = & \{\gamma \in \Gamma : \gamma X(t) = X(t) \quad \forall t\} \\ H & = & \{\gamma \in \Gamma : \gamma\{X(t)\} = \{X(t)\}\} \end{array} \tag{4.1}$$

The subgroup K is the group of *spatial symmetries* of $X(t)$ and the subgroup H of *spatiotemporal symmetries* consists of those symmetries that preserve the trajectory of $X(t)$. Suppose that $h \in H$. Then by uniqueness of solutions $hX(t) = X(t+\theta)$ for some phase shift $\theta \in \mathbf{S}^1$. The pair (h, θ) is also called a *spatiotemporal symmetry* of $X(t)$.

Let

$$L_K = \bigcup_{\gamma \in H \backslash K} \mathrm{Fix}(\gamma) \tag{4.2}$$

Theorem 4.1 (H/K Theorem [4, 9]) *Let Γ be a finite group acting on $\mathbf{R}^n$. There is a periodic solution to some Γ-equivariant system of ODE on $\mathbf{R}^n$ with spatial symmetries K and spatio-temporal symmetries H if and only if*

(a) *H/K is cyclic.*

(b) *K is an isotropy subgroup.*

(c) $\dim \mathrm{Fix}(K) \geq 2$. *If* $\dim \mathrm{Fix}(K) = 2$, *then either $H = K$ or $H = N(K)$.*

(d) *H fixes a connected component of* $\mathrm{Fix}(K) - L_K$.

Moreover, when these conditions hold, there exists a smooth Γ-equivariant vector field with an asymptotically stable limit cycle with the desired symmetries.

A Three-Cell Ring Coupled to a Two-Cell Ring

We start with an illustrative example of a multirhythm. Consider the five-cell network consisting of a unidirectional ring of three-cells and a bidirectional ring of two cells pictured in Figure 8. The cells in the three-cell ring are assumed to be different from those in the two-cell ring. Hence the differential equations are assumed to be unrelated, so the general system of differential equations associated with this network has the form:

$$\begin{array}{rcl} \dot{x_1} & = & f(x_1, x_2, x_3, \overline{y_1, y_2}) \\ \dot{x_2} & = & f(x_2, x_3, x_1, \overline{y_1, y_2}) \\ \dot{x_3} & = & f(x_3, x_1, x_2, \overline{y_1, y_2}) \\ \dot{y_1} & = & g(y_1, y_2, \overline{x_1, x_2, x_3}) \\ \dot{y_2} & = & g(y_2, y_1, \overline{x_1, x_2, x_3}) \end{array} \tag{4.3}$$

Here the bars indicate that f is symmetric in the y_j and g is symmetric in the x_j, that is,

$$f(x_1, x_2, x_3, y_1, y_2) = f(x_1, x_2, x_3, y_2, y_1)$$
$$g(y_1, y_2, x_1, x_2, x_3) = g(y_1, y_2, x_2, x_1, x_3) = g(y_1, y_2, x_2, x_3, x_1)$$

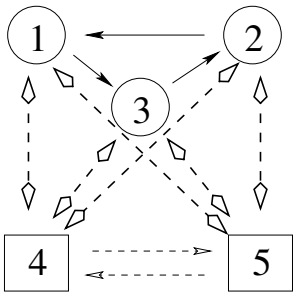

Figure 8: Five-cell system made of a ring of three and a ring of two.

Inspection of either the network architecture in Figure 8 or the cell system in (4.3) shows that these equations have symmetry group

$$\Gamma = \mathbf{Z}_3(\rho) \times \mathbf{Z}_2(\kappa) \cong \mathbf{Z}_6$$

where $\rho = (1\ 2\ 3)$ and $\kappa = (4\ 5)$ are cell permutations.

We will use the H/K theorem (Theorem 4.1) to show that systems of differential equations of the form (4.3) can produce multirhythms. Observe that (4.3) is the general $\mathbf{Z}_6$-equivariant vector field on the five-cell state space. In particular, we look for a periodic solution

$$X(t) = (x_1(t), x_2(t), x_3(t), y_1(t), y_2(t))$$

to (4.3) with symmetry $(H, K) = (\mathbf{Z}_6, \mathbf{1})$. Without loss of generality we may assume that $X(t)$ is a 1-periodic solution. First, we show that such a solution is a multirhythm, then we show that the H/K theorem implies that such a solution exists, and finally we discuss how one might find a system with such a solution (it cannot arise as a primary branch through an equivariant Hopf bifurcation).

Solution symmetry is equivalent to multirhythms. By assumption on (H, K) the periodic solution $X(t)$ has the spatiotemporal symmetry

$$\tau = ((1\ 2\ 3)(4\ 5), \tfrac{1}{6}),$$

Therefore $X(t)$ has the symmetries

$$\tau^2 = ((1\ 2\ 3), \tfrac{1}{3}) \qquad \tau^3 = ((4\ 5), \tfrac{1}{2})$$

The τ^2 symmetry forces the x_j to be a discrete rotating wave. The τ^3 symmetry forces the y_i to be a half-period out of phase with each other. Thus

$$X(t) = (x(t), x(t + \tfrac{1}{3}), x(t + \tfrac{2}{3}), y(t), y(t + \tfrac{1}{2}))$$

This solution is a multirhythm, because three times the frequency of y is equal to twice the frequency of x. (In detail: τ^3 symmetry implies that $x(t) = x(t + \frac{1}{2})$, and τ^2 symmetry implies that $y(t) = y(t + \frac{1}{3})$. So the period of $x(t)$ is $\frac{1}{2}$ and the period of $y(t)$ is $\frac{1}{3}$, so the ratio of the periods is 3/2, a multirhythm.)

H/K **Theorem implies existence of multirhythms.** We now give the existence proof. The phase space of (4.3) is $P = (\mathbf{R}^k)^3 \times (\mathbf{R}^l)^2$. Since every $\mathbf{Z}_6$-equivariant vector field on P is of the form (4.3), Theorem 4.1 states that a periodic solution $X(t)$ with the desired spatiotemporal symmetry exists in the family (4.3) if the pair $(\mathbf{Z}_6, \mathbf{1})$ satisfies (a)-(d). It is straightforward to check that (a)-(c) are satisfied. We claim that (d) is also valid when $l \geq 2$. To verify this point, observe that

$$L_{\mathbf{1}} = \{(x, x, x, y_1, y_2)\} \cup \{(x_1, x_2, x_3, y, y)\}$$

so that hence $\mathrm{codim}(L_{\mathbf{1}}) = \min\{2k, l\} > 1$. In particular, $P \setminus L_{\mathbf{1}}$ is connected, so under the assumption $l \geq 2$, condition (d) is automatically satisfied. Note that (d) fails when $l = 1$.

Multirhythms are secondary states in five-cell network. We now know that the required periodic solution exists. However, there is a difficulty in actually finding that solution, since no such solution is supported by a primary Hopf bifurcation in this coupled cell system. Specifically, the equivariant Hopf theorem [11, 9] implies that a periodic solution with $(\mathbf{Z}_6, \mathbf{1})$ symmetry can appear from a Hopf bifurcation in a Γ-equivariant system only if some subgroup of Γ has a two-dimensional irreducible representation in P whose effective action is the standard action of $\mathbf{Z}_6$ on $\mathbf{R}^2$. It is straightforward to verify that the action of $\Gamma = \mathbf{Z}_3 \times \mathbf{Z}_2$ on P has no such irreducible representation.

There does, however, exist a more complicated bifurcation scenario that contains such a representation: primary Hopf bifurcation to a $\mathbf{Z}_3$ discrete rotating wave, followed by a secondary Hopf bifurcation using the nontrivial $\mathbf{Z}_2$ representation. We present a numerical example of a 3:2 resonant solution arising by such a scenario. Let $x_1, x_2, x_3 \in \mathbf{R}$ be the state variables for the ring of three cells and let $y_1 = (y_1^1, y_2^1), y_2 = (y_1^2, y_2^2) \in \mathbf{R}^2$ be the state variables for the ring of two cells. Consider the system of ODE

$$\begin{array}{rcl}
\dot{x}_1 &=& -x_1 - x_1^3 + 2(x_1 - x_2) + D(y_1 + y_2) + 3((y_2^1)^2 + (y_2^2)^2) \\
\dot{x}_2 &=& -x_2 - x_2^3 + 2(x_2 - x_3) + D(y_1 + y_2) + 3((y_2^1)^2 + (y_2^2)^2) \\
\dot{x}_3 &=& -x_3 - x_3^3 + 2(x_3 - x_1) + D(y_1 + y_2) + 3((y_2^1)^2 + (y_2^2)^2) \\
\dot{y}_1 &=& B_1 y_1 - |y_1|^2 y_1 + B_2 y_2 + 0.4(x_1^2 + x_2^2 + x_3^2)C \\
\dot{y}_2 &=& B_1 y_2 - |y_2|^2 y_2 + B_2 y_1 + 0.4(x_1^2 + x_2^2 + x_3^2)C
\end{array} \tag{4.4}$$

where

$$B_1 = \begin{pmatrix} -\frac{1}{2} & 1 \\ -1 & -\frac{1}{2} \end{pmatrix} \quad B_2 = \begin{pmatrix} -1 & -1 \\ 1 & -1 \end{pmatrix} \quad D = (0.20, -0.11) \quad C = \begin{pmatrix} 0.10 \\ 0.22 \end{pmatrix}.$$

Starting at the initial condition

$$x_1^0 = 1.78 \quad x_2^0 = -0.85 \quad x_3^0 = -0.08 \quad y_1^0 = (-0.16, 0.79) \quad y_2^0 = (0.32, -0.47)$$

We obtain the numerical solution shown in Figures 9 and 10. Additional examples of multirhythms are presented in [9].

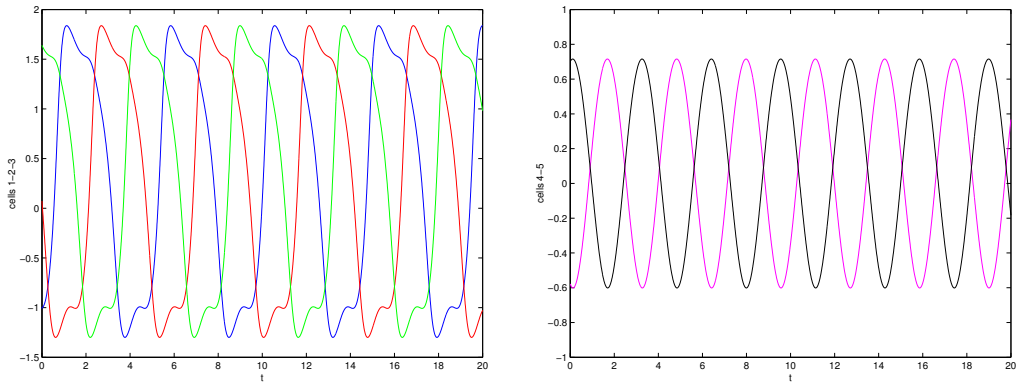

Figure 9: Integration of (4.3). (Left) Cells 1-2-3 out of phase by one-third period; (right) cells 4-5 out of phase by one-half period.

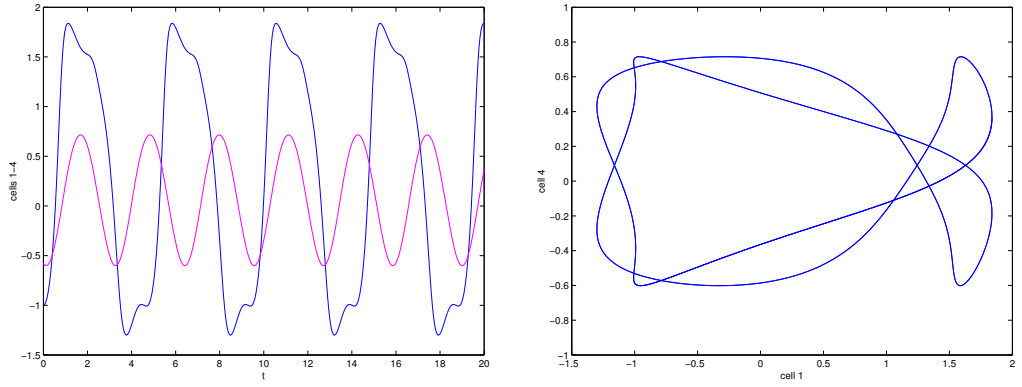

Figure 10: Integration of (4.3). (Left) Time series of cells 1 and 4 indicating that triple the frequency of cell 4 equals double the frequency of cell 1; (right) plot of cell 1 versus cell 4 showing a closed curve that indicates a time-periodic solution.

A p-Cell Ring Coupled to a q-Cell Ring

We end this section by generalizing the previous example to a class of networks that shows that all possible multirhythms can occur as rotating waves in a network composed of two coupled rings. Suppose that p and q are coprime with $p > q$. Consider a network consisting of unidirectional rings of size p and q, where each cell is one ring is coupled equally to all cells in the other ring, as illustrated in Figure 8 for $(p, q) = (3, 2)$. This network, whose phase space is $P = (\mathbf{R}^k)^p \times (\mathbf{R}^l)^q$, has symmetry group $\mathbf{Z}_{pq} \cong \mathbf{Z}_p \times \mathbf{Z}_q$.

Assume that either $q > 2$ or $l > 1$. Then periodic solutions with $H = \mathbf{Z}_{pq}$ and $K = \mathbf{1}$ can exist (for suitable choices of the vector field) by the H/K theorem, since the form of the coupled cell system is the general $\mathbf{Z}_{pq}$-equivariant vector field. We may assume that such a solution has period 1. As in the $(p, q) = (3, 2)$ case, symmetry implies that the solution is a discrete rotating wave in each ring. The p ring output has frequency $1/q$ and the q ring output has frequency $1/p$, which yields the frequency ratio p/q.

5 Three-Cell Feed-Forward Network: Periodic

We now discuss the linearizations of coupled cell systems about synchronous equilibria, showing that the normal forms can have unusual features. In this section we consider the three-cell feed-forward network illustrated in Figure 11. We observe that one-parameter synchrony-breaking leads naturally to nilpotent normal forms in these networks and to solutions that are equilibria in cell 1 and periodic in cells 2 and 3. Surprisingly, for a large class of bifurcations in these coupled cell systems, the amplitude growth of the periodic signal in cell 3 is to the power $\frac{1}{6}$ rather than the expected $\frac{1}{2}$ power of amplitude growth with respect to the bifurcation parameter in Hopf bifurcation.

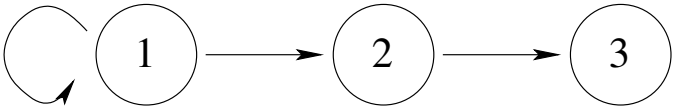

Figure 11: Three-cell linear feed-forward network.

This network has a feature that is not present in the previous networks — the first cell is coupled (externally) to itself [12] though, in fact, this point is not crucial. The coupled cell systems corresponding to this three-cell network have the form:

$$\begin{array}{rcl} \dot{x}_1 &=& f(x_1, x_1) \\ \dot{x}_2 &=& f(x_2, x_1) \\ \dot{x}_3 &=& f(x_3, x_2) \end{array} \tag{5.1}$$

A special codimension one synchrony-breaking Hopf bifurcation. We assume that the feed-forward coupled cell system (5.1) is in normal form in the sense of (5.3) below. We then prove that the generic one-parameter nilpotent Hopf bifurcation of the type governed by (5.2) leads to a periodic motion in cell 3 with period identical to that of cell 2.

We begin by assuming that the internal dynamics for each cell is two-dimensional and that $(0, 0, \lambda)$ is a stable equilibrium for

$$\dot{x}_1 = f(x_1, x_1, \lambda)$$

The Jacobian at the equilibrium $(0, 0, 0)$ for (5.1) has the form

$$\begin{bmatrix} A+B & 0 & 0 \\ B & A & 0 \\ 0 & B & A \end{bmatrix} \tag{5.2}$$

where $A = D_u f(0, 0, \lambda)$ is the linearized internal cell dynamics and $B = D_v f(0, 0, \lambda)$ is the linearized coupling. We assume, as above, that $A + B$ has eigenvalues with negative real part. Next we assume that that there is a Hopf bifurcation for cell 2 at $\lambda = 0$; that is, A has purely imaginary eigenvalues at $\lambda = 0$. It follows from (5.2) that purely imaginary

eigenvalues of A have multiplicity two as eigenvalues of the Jacobian. It is straightforward to arrange for the equation

$$\dot{x}_2 = f(x_2, 0, \lambda)$$

to have a unique stable limit cycle when $\lambda > 0$. With these assumptions cell 1 has an asymptotically stable equilibrium at the origin and cell 2 has a small amplitude stable limit cycle.

Next we assume that f is in 'normal form' for Hopf bifurcation in the following sense. We can identify the two-dimensional phase space of each cell with $\mathbf{C}$; then the $\mathbf{S}^1$-equivariance of normal form implies

$$f(e^{i\theta}u, e^{i\theta}v) = e^{i\theta}f(u, v) \tag{5.3}$$

More specifically,

$$f(u, v, \lambda) = a(|v|^2, \overline{v}u, |u|^2, \lambda)u + b(|v|^2, v\overline{u}, |u|^2, \lambda)v \tag{5.4}$$

where a and b are complex-valued functions. Note that this is *not* the normal form for the nilpotent Hopf bifurcation that occurs in the feed-forward system; so it is a special assumption.

Proposition 5.1 *Suppose that (5.1) has two-dimensional internal dynamics f of the form (5.4). Suppose that a synchrony-breaking Hopf bifurcation occurs in cell 2 as the bifurcation parameter λ is varied through 0; that is,*

$$\begin{array}{rcl} \mathrm{Re}(a(0)) & = & 0 \\ \mathrm{Re}(a_\lambda(0)) & > & 0 \end{array} \tag{5.5}$$

In addition, make the stability assumptions

$$\begin{array}{rcl} \mathrm{Re}(b(0)) & < & 0 \\ \mathrm{Re}(a_3(0)) & < & 0 \end{array} \tag{5.6}$$

Then there is a unique supercritical branch of asymptotically stable periodic solutions emanating from this bifurcation with the first cell being in equilibrium and the periods of cells 2 and 3 being equal. The amplitude of the periodic state in cell 2 grows as $\lambda^{\frac{1}{2}}$; the amplitude of cell 3 grows as $\lambda^{\frac{1}{6}}$.

Proof By (5.4) the origin in the first cell equation

$$\dot{x}_1 = f(x_1, x_1)$$

is linearly stable if $\mathrm{Re}(b(0) + a(0)) < 0$ which follows from (5.5) and (5.6). Thus we can assume $x_1 = 0$.

The cell 2 equation

$$\dot{x}_2 = f(x_2, 0) = a(0, 0, |x_2|^2)x_2$$

has a Hopf bifurcation at the origin, since $\mathrm{Re}(a(0)) = 0$, and a branch of periodic solutions emanates from this bifurcation, since $\mathrm{Re}(a_\lambda(0)) > 0$. The branch of periodic solutions produced by Hopf bifurcation in the cell 2 equation is supercritical and stable, since $\mathrm{Re}(a_3(0)) < 0$.

Under these assumptions (see (5.2)) the center subspace at this bifurcation is the four-dimensional subspace $\{(0, x_2, x_3)\}$, the purely imaginary eigenvalues are each double, and the linearization is nilpotent (since $b(0) \neq 0$). Moreover, the skew product nature of (5.1) guarantees that this subspace is flow-invariant and hence a center manifold. The vector field on this center manifold is

$$\dot{x}_2 = a(0, 0, |x_2|^2, \lambda)x_2 \tag{5.7}$$

$$\dot{x}_3 = b(|x_2|^2, x_2\overline{x_3}, |x_3|^2, \lambda)x_2 + a(|x_2|^2, \overline{x_2}x_3, |x_3|^2, \lambda)x_3 \tag{5.8}$$

where λ is the Hopf bifurcation parameter.

Since (5.7) is in normal form, the periodic solutions that emanate from this bifurcation have circles $|x_2| = r$ as trajectories. The constant $r(\lambda)$ is found by solving

$$\mathrm{Re}(a(0, 0, r^2, \lambda)) = 0$$

and $r(\lambda)$ is of order $\sqrt{\lambda}$. Set $\omega(\lambda) = \mathrm{Im}(a(0, 0, r^2(\lambda), \lambda))$. Then the bifurcating periodic solution is

$$x_2(t) = r(\lambda)e^{i\omega(\lambda)t} \tag{5.9}$$

where $\omega(0) = \mathrm{Im}(a(0))$.

Using the feed-forward skew product character of the equations, we can insert (5.9) into (5.8) to analyze x_3. To investigate $x_3(t)$ when $\lambda > 0$ we write

$$x_3 = \frac{1}{r}x_2 y$$

which defines $y(t)$ implicitly. Now $|x_2|^2 = r^2$, $\overline{x_2}x_3 = ry$, and $|x_3|^2 = |y|^2$.

We now derive the differential equation (5.10) for y. Using (5.7) compute

$$\dot{x}_3 = \frac{1}{r}(\dot{x}_2 y + x_2\dot{y}) = \frac{1}{r}(cx_2 y + x_2\dot{y})$$

where $c(|x_2|^2, \lambda) = a(0, 0, |x_2|^2, \lambda)$. Note that on substitution of (5.9) $c = i\omega(\lambda)$. On the other hand, (5.8) implies

$$\dot{x}_3 = bx_2 + \frac{1}{r}ax_2 y.$$

Equating the two expressions for $\dot{x}_3$ and dividing by x_2/r, we obtain

$$\dot{y} = rb(r^2, r\bar{y}, |y|^2, \lambda) + (a(r^2, r\bar{y}, |y|^2, \lambda) - i\omega(\lambda))y \equiv g(y, \lambda) \tag{5.10}$$

If (5.10) has a stable equilibrium (as a function of λ) in a neighborhood of the origin, then cell 3 will be periodic with the same frequency as cell 2.

Next we show that the amplitude of the periodic state in cell 3 grows as $\lambda^{\frac{1}{6}}$, and we verify the stability statement. Indeed, we show that there exists a unique branch of stable equilibria to (5.10) emanating from $y = 0$ at $\lambda = 0$. To do this, rescale $g = 0$ in (5.10) by setting $s = \lambda^{\frac{1}{6}}$ and $y = su$ to obtain

$$s^3\widetilde{b}(s^6\rho^2, s^4\rho\bar{u}, s^2|u|^2, s^6) + \widetilde{a}(s^6\rho^2, s^4\rho\bar{u}, s^2|u|^2, s^6)su = 0 \tag{5.11}$$

where $r(\lambda) = s^3\rho(s^6)$, $\widetilde{b} = \rho b$, and $\widetilde{a} = a - i\omega$. Note that $\widetilde{b}(0) \neq 0$ and $\widetilde{a}(0) = 0$.

We use the implicit function theorem to show that there is a unique branch of zeros of (5.11) as a function u of s^2. Dividing by s, expanding in powers of s^2, and then dividing again by s^2, we obtain

$$h(u, s) = \widetilde{b}(0) + \widetilde{a}_3(0)|u|^2u + \mathcal{O}(s^2) = 0$$

We make the genericity hypothesis that

$$a_3(0) = \widetilde{a}_3(0) \neq 0 \tag{5.12}$$

There is a unique $u_0 \in \mathbf{C}$ for which

$$\widetilde{b}(0) + a_3(0)|u_0|^2u_0 = 0$$

and this implies that $u_0 \neq 0$. Thus $h(u_0, 0) = 0$. Next calculate at $s = 0$

$$(dh)w = a_3(0)(2|u|^2w + u^2\bar{w}) \tag{5.13}$$

Therefore at u_0 we have

$$(dh)w = a_3(0)(2|u_0|^2w + u_0^2\bar{w})$$

and thus

$$\det(dh) = 3|a_3(0)|^2|u_0|^4 > 0$$

The implicit function theorem now implies that there is a unique branch of equilibria at which

$$y_0(\lambda) = su(s^2) = \lambda^{\frac{1}{6}}u_0 + \mathcal{O}(\sqrt{\lambda}) \tag{5.14}$$

since $s^3 = \sqrt{\lambda}$.

Note that

$$\mathrm{tr}(dh) = 4\,\mathrm{Re}(a_3(0))|u_0|^2 + \mathcal{O}(s^2)$$

Since $\mathrm{Re}(a_3(0)) < 0$, the branch of equilibria of (5.10) is asymptotically stable. □

A simple example of a function $f : \mathbf{C}^2 \times \mathbf{R} \to \mathbf{C}$ that satisfies the hypotheses of Proposition 5.1 is

$$f(u, v, \lambda) = (i + \lambda)u - |u|^2u - v \tag{5.15}$$

The resulting periodic solution is shown in Figure 12.

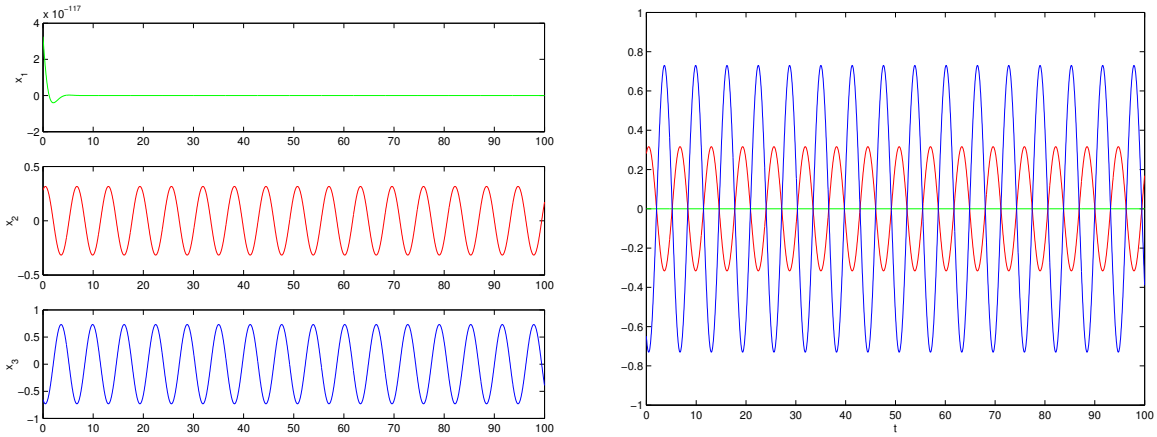

Figure 12: Time series from three-cell network with f as in (5.15) and $\lambda = 0.1$: (left) first coordinate time series of individual cells; (right) superimposed time series from all three cells. Note that $\sqrt{\lambda} = 0.32$ and $\lambda^{1/6} = 0.68$ and that these values are the approximate amplitudes of the periodic states in cells 2 and 3 respectively.

Comments on a general synchrony-breaking Hopf theorem. We conjecture that the results of Proposition 5.1 are valid generally, and not just for coupled cell systems in the 'normal form' (5.4). Several steps are needed to reduce the feed-forward system to a vector field on a four-dimensional center manifold that has structure similar to that of (5.4). We must show that at bifurcation the feed-forward system reduces to a vector field on a four-dimensional center manifold with similar structure to (5.4). In the next subsection we present a partial result in this direction, namely, that the vector field on the center manifold can always be assumed to have skew product form. We are not able to show that the vector field can be reduced by normal form techniques to the form (5.4); so we connot obtain an analogue of equation (5.10), which is central to the proof of Proposition 5.1.

Center manifold reduction and skew products. The next lemma shows that the skew product form of (5.1) implies a skew product form for a corresponding center manifold reduction. Consider the skew product vector field

$$\begin{array}{lrcl} (a) & \dot{x} & = & F(x) \\ (b) & \dot{y} & = & G(x,y) \end{array} \tag{5.16}$$

where $x \in \mathbf{R}^k$, $y \in \mathbf{R}^\ell$, $F : \mathbf{R}^k \to \mathbf{R}^k$, and $G : \mathbf{R}^k \times \mathbf{R}^\ell \to \mathbf{R}^\ell$.

Suppose that (x_0, y_0) is an equilibrium of (5.16) with center subspace $E^c \subset \mathbf{R}^k \times \mathbf{R}^\ell$. Then x_0 is an equilibrium of (5.16)(a); suppose that the center subspace at this equilibrium is $E^c_x \subset \mathbf{R}^k$. Let

$$\pi : \mathbf{R}^k \times \mathbf{R}^\ell \to \mathbf{R}^k$$

be projection. Then $\pi(E^c) = E^c_x$. More precisely, the linearization L of (5.16) at (x_0, y_0) has

the form

$$L = \begin{bmatrix} (d_x F)_{x_0} & 0 \\ * & (d_y G)_{(x_0,y_0)} \end{bmatrix}$$

so the critical eigenvalues of L are those of the matrices $(d_x F)_{x_0}$ and $(d_y G)_{(x_0,y_0)}$. We can write

$$E^c = E_F \oplus E_G$$

where E_F is spanned by the generalized eigenvectors of L corresponding to critical eigenvalues of $(d_x F)_{x_0}$, E_G is the center subspace of $(d_y G)_{(x_0,y_0)}$, and $\pi|_{E_F} : E_F \to E_x^c$ is an isomorphism.

Lemma 5.2 *Let $\mathcal{N}$ be a center manifold for (5.16)(a) at x_0. Then:*

(a) *There exists a center manifold $\mathcal{M}$ for (5.16) at (x_0, y_0) such that $\mathcal{N} = \pi(\mathcal{M})$.*

(b) *The center manifold vector field on $\mathcal{M}$ may be pulled back to $E_x^c \oplus E_G$ so that it is in skew product form.*

Proof The flow ψ_t of the skew product system (5.16) has the form

$$\psi_t(x, y) = (\psi_t^x(x), \psi_t^y(x, y))$$

so $\pi \circ \psi_t = \psi_t^x$.

(a) Note that $\pi^{-1}(\mathcal{N}) = \mathcal{N} \times \mathbf{R}^\ell$ is a flow-invariant submanifold for (5.16). Let $\mathcal{M}$ be a center manifold for (5.16) in $\pi^{-1}(\mathcal{N})$ at (x_0, y_0). Since $\pi|_{\mathcal{M}}(E_F) = E_x^c$, this map is a submersion. Therefore locally $\pi(\mathcal{M}) = \mathcal{N}$.

(b) Consider the submersion $\pi|_{\mathcal{M}} : \mathcal{M} \to \mathcal{N}$. The manifold $\mathcal{M}$ is a bundle over $\mathcal{N}$ with bundle map $\pi|_{\mathcal{M}}$. Thus $\pi|_{\mathcal{M}}$ commutes with the flows on the center manifolds $\mathcal{M}$ and $\mathcal{N}$. Hence $d\pi|_{\mathcal{M}}$ is constant on the $\mathcal{M}$ center manifold vector field V restricted to a fiber. Locally, V can be put in skew product form. □

6 Feed-Forward Networks: Quasiperiodic States

Feed-forward networks illustrate another strange feature of network dynamics: the occurrence of very different states in different cells. We show by numerical example that there are coupled cell systems in the three-cell feed-forward network with solutions that exhibit different forms of dynamic behavior in each of the three cells. In particular, there are solutions $x(t) = (x_1(t), x_2(t), x_3(t))$ where $x_1(t)$ is an equilibrium, $x_2(t)$ is time periodic, and $x_3(t)$ is quasiperiodic. The time series from such a cell system is presented in Figure 13. The specific function f used in this simulation is:

$$f(u, v) = (i + \lambda - |u|^2)u - v - \frac{1}{\sqrt{\lambda}}|v|^2 v + \left(\frac{1 + \sqrt{2}i}{\lambda} - 1\right)|v|^2 u \tag{6.1}$$

where $u, v \in \mathbf{C}$, λ is a parameter, and we take $\lambda = 0.3$.

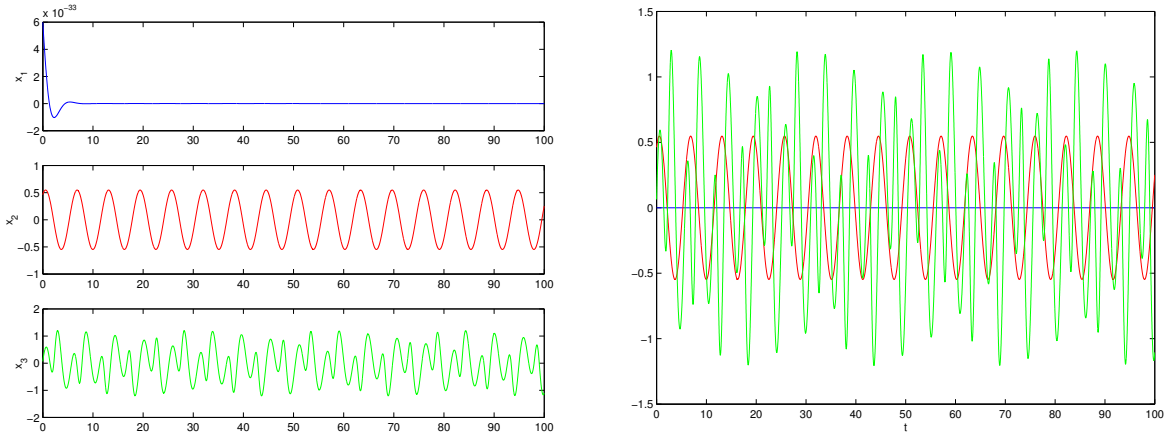

Figure 13: Time series from three-cell network in Figure 11 using (6.1): (left) first coordinate time series of individual cells; (right) superimposed time series from all three cells.

We now discuss how to find a function f like the one in (6.1) so that the ODE (5.1) exhibits the desired dynamics. As in Section 5 we assume that f is in 'normal form' (5.3) and we assume that the Hopf bifurcation in the cell 2 equation is also in standard form, that is,

$$f(x_2, 0, \lambda) = a(0, 0, |x_2|^2, \lambda)x_2 = (i + \lambda - |x_2|^2)x_2 \tag{6.2}$$

Then we analyze the equation

$$\dot{x}_3 = f(x_3, x_2)$$

By (6.2)

$$x_2 = \sqrt{\lambda}e^{it}$$

Next, we write

$$x_3 = yx_2$$

and derive the following equation for y

$$\dot{y} = rb(r^2, r\bar{y}, |y|^2, \lambda) + (a(r^2, r\bar{y}, |y|^2, \lambda) - i)y \tag{6.3}$$

where $a(0) = i$, $r^2 = \lambda$, and (to ensure stability of the origin in cell 1) $b(0) = -1$.

The final step is to guarantee that (6.3) has a stable periodic solution (with irrational frequency). Then $x_3(t)$ will exhibit two-frequency quasiperiodic motion. The periodic solution y in (6.3) is found by varying a second parameter so that the sign of $\mathrm{Re}(a_3(0))$ changes. This leads to a Hopf bifurcation in the y equation and (depending on higher order terms) to stable quasiperiodic motion in cell 3. The example that began this section was constructed using this approach. We have not resolved whether generically in two-parameter systems quasiperiodic states or phase-locked states or both can be expected in cell 3. This is a question of resonance tongues.

A feed-forward network with four cells. It is natural to consider the dynamics of an n-cell feed-forward network of the form:

$$\begin{aligned} \dot{x}_1 &= f(x_1, x_1) \\ \dot{x}_2 &= f(x_2, x_1) \\ &\vdots \\ \dot{x}_n &= f(x_n, x_{n-1}) \end{aligned} \tag{6.4}$$

with the function f as in Section 5, specifically in (6.1).

Numerical investigations suggest that each added cell contributes to the complexity of the dynamics. For example, when $n = 4$, x_1 is an equilibrium, x_2 is periodic, x_3 is two-frequency quasiperiodic, and x_4 is again two-frequency, but in a more complicated and curious way. See Figure 14.

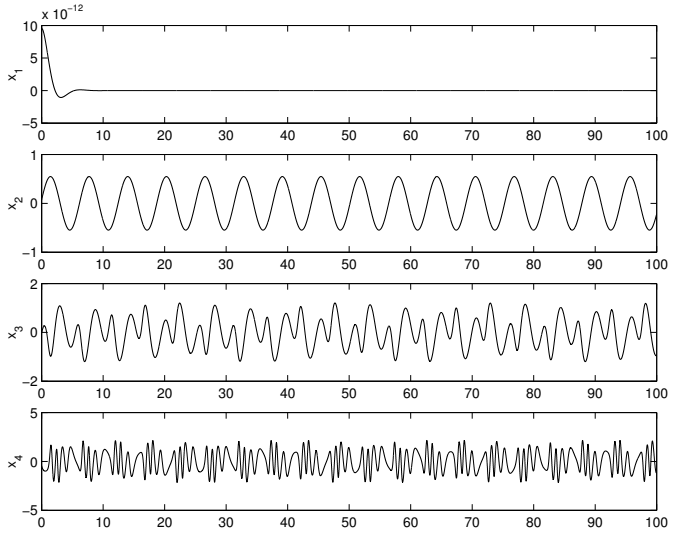

Figure 14: Time series for first coordinate in each cell of a four-cell feed-forward network using (6.1).

To check that cells 3 and 4 display two-frequency quasiperiodicity we sample x_3 and x_4 at each period of cell 1. The results of this stroboscopic map are shown in Figure 15 where the sampled orbits of x_3 trace out a circle and the sampled orbits of x_4 trace out a circle that winds three times around the origin. It is perhaps surprising that the dynamics of cell 4 is quasiperiodic with one period given by the period in cell 2. Further analysis is needed to determine whether this phenomenon is genuine (rather than a numerical artifact), and if so, whether it is robust or typical. Again, the issue of resonance tongues is an important one.

7 Nilpotent Normal Forms

In Section 5 we observed that synchrony-breaking bifurcations in feed-forward chains lead naturally to nilpotent normal forms in codimension-one bifurcations. See (5.2). Perhaps

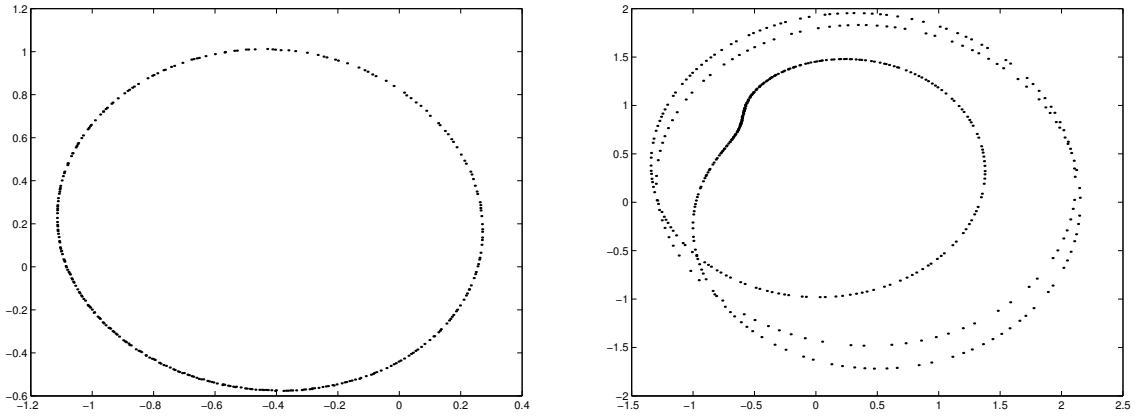

Figure 15: Stroboscopic map for (6.4) based on the time series in Figure 14. The positions of cell 3 (left) and cell 4 (right) are plotted after each period of cell 2.

surprisingly, synchrony-breaking can lead to nilpotent normal forms for a variety of network architectures, including ones that are not feed-forward. An example is the five-cell ring in Figure 16. (A similar five-cell network is considered in [13].)

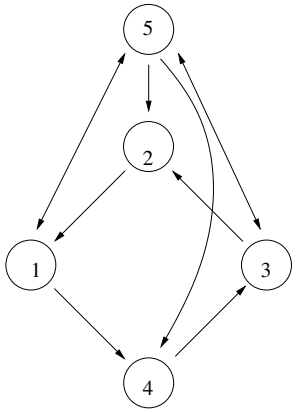

Figure 16: Five-cell ring that leads to nilpotent normal forms in synchrony-breaking bifurcations.

Since the five-cell system consists of identical cells, the k-dimensional diagonal subspace

$$D = \{x \in (\mathbf{R}^k)^5 : x_1 = x_2 = x_3 = x_4 = x_5\}$$

is flow-invariant. This five-cell system has a true symmetry

$$\tau = (1\ 3)(2\ 4)$$

so the $3k$-dimensional subspace

$$\mathrm{Fix}(\tau) = \{x \in (\mathbf{R}^k)^5 : x_1 = x_3; x_2 = x_4\}$$

is also flow-invariant. Note that coloring cells 1 to 4 one color and cell 5 another is a balanced relation. Therefore, the $2k$-dimensional subspace

$$W = \{x \in (\mathbf{R}^k)^5 : x_1 = x_2 = x_3 = x_4\}$$

is flow-invariant.

Let $X_0 = (x_0, x_0, x_0, x_0, x_0)$ be a synchronous equilibrium. Let A be the $k \times k$ matrix obtained by linearizing the internal dynamics at x_0, and let B be the $k \times k$ matrix of linearized couplings at X_0. Then the Jacobian matrix at X_0 has the form

$$J = \begin{bmatrix} A & B & 0 & 0 & B \\ 0 & A & B & 0 & B \\ 0 & 0 & A & B & B \\ B & 0 & 0 & A & B \\ B & 0 & B & 0 & A \end{bmatrix}$$

The subspaces

$$D \subset W \subset \mathrm{Fix}(\tau)$$

are therefore invariant subspaces for J. Moreover, the $2k$-dimensional subspace

$$U = \{x \in (\mathbf{R}^k)^5 : x_3 = -x_1; x_4 = -x_2; x_5 = 0\}$$

is J-invariant.

To simplify notation, let $k = 1$. Using these invariant subspaces we choose a basis for $\mathbf{R}^5$ that puts J in normal form. Let

$$e_1 = \begin{bmatrix} 1 \\ 1 \\ 1 \\ 1 \\ 1 \end{bmatrix} \quad e_2 = \begin{bmatrix} 1 \\ 1 \\ 1 \\ 1 \\ -2 \end{bmatrix} \quad e_3 = \frac{3}{2}\begin{bmatrix} 1 \\ -1 \\ 1 \\ -1 \\ 0 \end{bmatrix} \quad e_4 = \begin{bmatrix} 1 \\ 0 \\ -1 \\ 0 \\ 0 \end{bmatrix} \quad e_5 = \begin{bmatrix} 0 \\ 1 \\ 0 \\ -1 \\ 0 \end{bmatrix}$$

so

$$\begin{aligned} Je_1 &= (A + 2B)e_1 \\ Je_2 &= (A - B)e_2 \\ Je_3 &= (A - B)e_3 + Be_1 - Be_2 \\ Je_4 &= Ae_4 - Be_5 \\ Je_5 &= Be_4 + Ae_5 \end{aligned}$$

In this basis J has the form

$$\begin{bmatrix} A + 2B & 0 & B & 0 & 0 \\ 0 & A - B & -B & 0 & 0 \\ 0 & 0 & A - B & 0 & 0 \\ 0 & 0 & 0 & A & B \\ 0 & 0 & 0 & -B & A \end{bmatrix}$$

Thus the $5k$ eigenvalues of J consist of the eigenvalues of the $k \times k$ matrix $A - B$ repeated twice, the eigenvalues of the $k \times k$ matrix $A + 2B$, and the eigenvalues of the $k \times k$ matrix $A+iB$ and their complex conjugates. Moreover, generically the double eigenvalues associated to the matrix $A - B$ have geometric multiplicity 1, that is, those eigenvalues correspond to a nilpotent Jordan form. It follows that it is possible to find a 1:1 resonant Hopf bifurcation with a nilpotent normal form occurring generically in codimension one. For example, let

$$B = -I_2 \quad \text{and} \quad A = B + \begin{bmatrix} 0 & -1 \\ 1 & 0 \end{bmatrix}$$

8 Coupled Rings

Finally we present simulation results in which two rings of cells, coupled asymmetrically through a 'buffer' cell, appear to exhibit rotating wave states with incommensurate frequencies. Close inspection suggests that these states lie on thin tori, not closed loops, so they are presumably quasiperiodic. (They cannot be precisely periodic with the apparent 'short' period.)

Specifically, we work with a network consisting of two unidirectional rings of identical cells of three and five cells respectively. Because just one cell from each ring is coupled to the buffer cell, this network has no symmetry. See Figure 17. The results of simulations are shown in Figure 18. The left panel indicates a solution that appears to be a periodic rotating wave in either ring, with distinct periods. Note the more complicated dynamics that is visible in the buffer cell. The right panel plots the time series of a cell in the left ring versus a cell in the right ring. This view shows that the solution in the nine-dimensional phase space is either periodic of long period, or quasiperiodic.

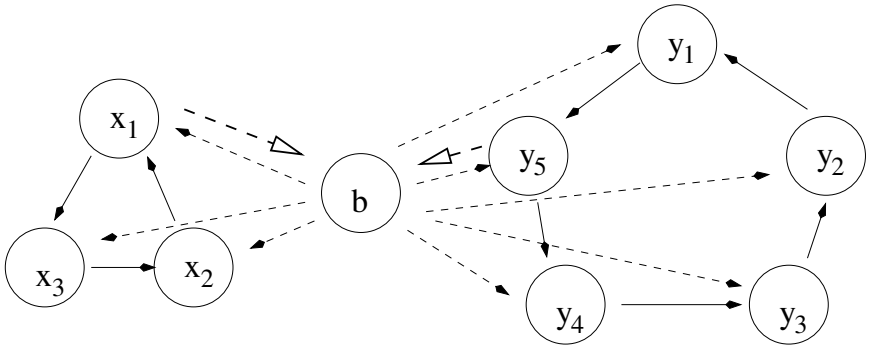

Figure 17: Unidirectional three and five-cell rings connected by a buffer cell.

The simulation is performed with the same one-dimensional internal dynamics in each cell, including the buffer cell, and with linear coupling. The internal dynamics is given by

$$g(u) = u - \tfrac{1}{10}u^2 - u^3$$

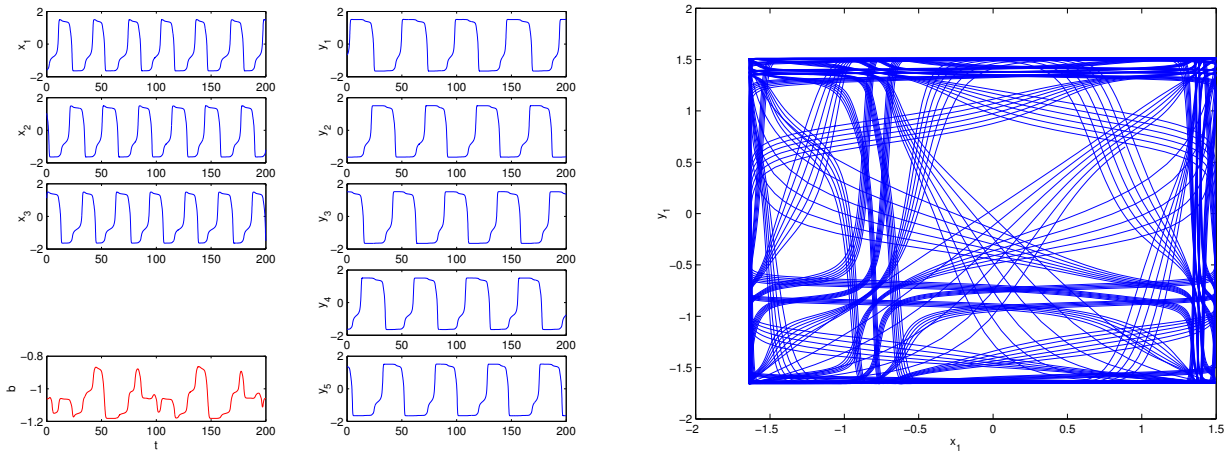

Figure 18: Simulation based on the network in Figure 17 using the differential equations in (8.1). (Left) time series from the nine cells; (right) x_1 versus y_1.

The differential equations with coupling are:

$$\begin{array}{rcll} \dot{x}_j & = & g(x_j) + 0.75(x_j - x_{j+1}) + 0.2\, b & j = 1, \ldots, 3 \\ \dot{b} & = & g(b) + 0.1(x_1 + y_5) & \\ \dot{y}_j & = & g(y_j) + 0.75(y_j - y_{j+1}) + 0.2\, b & j = 1, \ldots, 5 \end{array} \tag{8.1}$$

where the indexing assumes that $x_4 = x_1$ and $y_6 = y_1$. We remark that solutions of the type that we describe here occur frequently in simulations in cell systems where each cell has one-dimensional internal dynamics.

9 Conclusions

This paper presents a collection of curious examples of coupled cell networks, revealing the *typical* presence of behavior that would not be expected in a generic dynamical system. It traces this 'exotic' behavior to various features of the network architecture—sometimes in full rigor and sometimes only through numerical evidence.

The implications of these examples are of two kinds. The first, perhaps rather negative, implication is that apparently harmless modeling assumptions about networks can introduce special dynamical features that may not be fully representative of alternative models that have just as much scientific validity. It makes sense to be aware of the pitfalls here. The second, more positive, implication is that networks make available many interesting kinds of dynamical behavior, in a generic manner, that would not occur in a typical unconstrained dynamical system. Nature, especially in evolutionary guise, can build on such behavior and exploit it. In short: the 'generic' dynamics of networks differs in important respects from that of comparably complex dynamical systems, even when the effects of symmetry are taken into account. Some of these differences are now understood, and many relate to

the groupoid 'symmetries' of the network. Others remain puzzling and must be explained in different ways. The classical theory of nonlinear dynamical systems remains a vital part of the toolkit required to understand network dynamics, but it must be wielded with caution.

Acknowledgments

We thank Andrew Török and Marcus Pivato for helpful conversations. We also thank the referees for their excellent comments and suggestions. The work of MG was supported in part by NSF Grants DMS-0071735 and DMS-0244529 and ARP Grant 003652-0032-2001. MN was supported in part by a grant from the Leverhulme Trust, NSF Grant DMS-0071735, and the Mathematics Department of the University of Houston.

References

[1] D. Armbruster and P. Chossat. Remarks on multi-frequency oscillations in (almost) symmetrically coupled oscillators. *Phys. Lett. A* **254** (1999) 269–274.

[2] P. Ashwin and J.W. Swift. The dynamics of n identical oscillators with symmetric coupling. *J. Nonlin. Sci.* **2** (1992) 69–108.

[3] E. Brown, P. Holmes, and J. Moehlis. Globally coupled oscillator networks. In: *Perspectives and Problems in Nonlinear Science: A Celebratory Volume in Honor of Larry Sirovich* (E. Kaplan, J. Marsden, and K.R. Sreenivasan, eds) Springer, 2003, 183–215.

[4] P.L. Buono and M. Golubitsky. Models of central pattern generators for quadruped locomotion: I. primary gaits. *J. Math. Biol.* **42** No. 4 (2001) 291–326.

[5] S. Chow, J. Mallet-Paret, and E. Van Vleck. Dynamics of lattice differential equations. *Int. Jnl. Bifur. Chaos.* **6** No. 9 (1996) 1605-1621.

[6] S. Chow, J. Mallet-Paret, and E. Van Vleck. Pattern formation and spatial chaos in spatially discrete evolution equations. *Random and Computational Dynamics* **4** (1996) 109-178.

[7] D. Gillis and M. Golubitsky. Patterns in square arrays of coupled cells. *J. Math. Anal. App.* **208** (1997) 487-509.

[8] M. Golubitsky and I. Stewart. Hopf bifurcation with dihedral group symmetry: coupled nonlinear oscillators, in *Multiparameter Bifurcation Theory* (M.Golubitsky and J.Guckenheimer eds.), Proceedings of the AMS-IMS-SIAM Joint Summer Research Conference, July 1985, Arcata; *Contemporary Math.* **56** Amer. Math. Soc., Providence RI, 1986, 131–173.

[9] M. Golubitsky and I. Stewart. *The Symmetry Perspective: From Equilibrium to Chaos in Phase Space and Physical Space*. Progress in Mathematics **200**, Birkhäuser, Basel, 2002.

[10] M. Golubitsky and I. Stewart. Patterns of oscillation in coupled cell systems. In: *Geometry, Dynamics, and Mechanics: 60th Birthday Volume for J.E. Marsden* (P. Holmes, P. Newton, and A. Weinstein, eds.) Springer-Verlag, 2002, 243–286.

[11] M. Golubitsky, I. Stewart, and D.G. Schaeffer. *Singularities and Groups in Bifurcation Theory II*, Applied Mathematics Sciences, **69**, Springer Verlag, New York, 1988.

[12] M. Golubitsky, I. Stewart, and A. Török. Patterns of synchrony in coupled cell networks with multiple arrows. Submitted.

[13] I. Stewart, M. Golubitsky, and M. Pivato. Patterns of synchrony in coupled cell networks. *SIAM J. Appl. Dynam. Sys.* To appear.

[14] Y. Wang and M. Golubitsky. Two-color patterns of synchrony in lattice dynamical systems. In preparation.